Original article

Retention profile of As (III) and As (V) oxyanions from water onto polypyrrole

Salman S. Alharthi

Department of Chemistry, College of Science, Taif University, P.O.Box 11099, Taif 21944, Saudi Arabia

ABSTRACT

An investigation on the use of polypyrrole (PPy) as a sorbing agent to remove As (III) and As (V) oxyanions from water is reported. The material was characterized by Fourier-transform infrared (FT-IR), thermo-gravimetric analysis (TGA), Brunauer–Emmett–Teller (BET), electrical conductivity and scanning electron microscopy (SEM). The interaction of As (III) and As (V) oxyanions with PPy was assessed by FT-IR and SEM-EDX. Effects of mass, pH and temperature for the removal of As (III) and As (V) from aqueous medium were optimized. The capacity of PPy to remove As (III) and As (V) oxyanions from water was found to be 15.58 and 16.67 mg g^{-1} respectively. The kinetic studies revealed fast removal mechanism which follows the pseudo-first order. PPy was tested for its efficiency to remove arsenic species from real water samples. The percentage of removal from these samples was 98%. The removal ability of PPy relative to previously reported materials for arsenic oxyanions sequestration from water is discussed.

1. Introduction

Arsenic has been classified as the most hazardous pollutant in the world. In 2001, the World Health Organization (WHO) has raised major environmental and toxicological awareness regarding different concentrations of this pollutant found in the groundwater of many countries around the world (Shankar and Shanker, 2014). The chronic exposure to arsenic either *via* contaminated drinking water or agricultural products irrigated with contaminated water can result in serious health issues such as cancers of liver, brain, kidney and stomach in addition to skin lesions and hyperkeratosis. Consequently, due to the pollutant toxicological effects, a standard value of MCL (maximum contaminant level) of 10 μg L^{-1} for arsenic in drinking water was adopted by the WHO (2010), the US-Environmental Protection Agency (US-EPA) and the European Commission (EC) (Smedley and Kinniburgh, 2002). Regarding the oxidation state, the pollutant can occur in four forms, arsenic (As (0)), arsine (AsH$_3$), arsenite (AsO$_3^{3-}$) and arsenate (AsO$_4^{3-}$).

In addition, organic forms of arsenic monomethylarsonic acid (CH$_3$AsO(OH)$_2$) and dimethylarsinic acid ((CH$_3$)$_2$AsO(OH)) were found as well in the natural water system, a main route of arsenic ingestion to humans. However, the inorganic trivalent form (As(III) as H$_3$AsO$_3$ and H$_2$AsO$_3^-$) is the most prevalent species in many ground waters due to the anoxic reducing conditions as it is more mobile and ten times more toxic than arsenate. Moreover, arsenite is almost seventy times more toxic than the methylated forms (CH$_3$AsO(OH)$_2$ and (CH$_3$)$_2$AsO(OH)) (Tyson, 2013). Great attention has been paid to develop cost-effective technologies to remove arsenic species from water. Technologies such as sorption techniques (Singh and Pant, 2004), co-precipitation (De Klerk et al., 2012), ion exchange (Barakat and Ismat-Shah, 2013), developed Mg-Fe-Cl LDH (Jiang et al., 2015), iron-coated sand (Herbel and Fendorf, 2006), membrane-based techniques including reverse osmosis (Capito et al., 2013) and nano-filtration (Xia et al., 2007), along with iron based materials (Litter et al., 2014) and activated carbon have been extensively used to remove the ionic species from water. Among these techniques, sorption method was extensively reported in the literature for arsenic ions removal from aqueous medium.

Polypyrrole (PPy) has been identified as one of the most attractive conductive electroactive polymer among various conducting materials. It is characterized by its high conductivity and environment stability (Chitte et al., 2011). Polymerization of pyrrole using ferric chloride in water is a fast reaction where insoluble black powder product is usually obtained. Studies have demonstrated the role of Iron (III) chloride in the yield of the PPy polymerization (Obidul Huq et al., 2018). Armes (1987) reported that

E-mail address: s.a.alharthi@tu.edu.sa

Peer review under responsibility of King Saud University.

Iron (III)/pyrrole molar ratio has no effect on the conductivity or the chemical composition of the product. Several investigations have been conducted on the analytical applications of nanocomposites or coated PPy (Wysocka-Zolopa et al., 2018; Yağmur, 2020). Obidul Huq et al reported the use of PPy in arsenic ions sorption with lower removal percentage 7.40 wt% for As^{3+} and removal capacity 1.91 mg/g for As^{5+} respectively (Obidul Huq et al., 2018). Nevertheless, the former study lacks the optimization process for maximal arsenic ions sequestration whereas the latter report did not tackle the application of the material in real wastewater samples. Ansari et al investigated the use of PPy, polyaniline and poly 3-methylthiophene coated with sawdust on the As^{3+} removal from water with 74.5, 82.6 and 85% arsenic removed (Ansari et al., 2008). Two studies have investigated the efficiency of modified PPy with nickel or greigite (Fe_3S_4) on As (III) and As (V) removal from water (Srivastava et al., 2016; Islam and Patel, 2017). However, relatively low capacities of these two PPy nanocomposites for arsenic ions were obtained.

In this paper a report on the structural characterization of PPy, its interaction with As (III) and As (V) *via* FT-IR and SEM-EDX analyzes, optimum conditions for the removal of investigated arsenic oxyanions (mass of the material, pH, kinetics and temperature) and the capacity of the material to sequester As (III) and As (V) from water are discussed. PPy effectiveness will be tested in real water samples.

2. Materials and Methods

2.1. Reagents and chemicals

Pyrrole (C_4H_4NH, 99%), Iron (III) chloride hexahydrate ($FeCl_3$·$6H_2O$, 97%), sodium arsenate dibasic heptahydrate (Na_2HAsO_4·$7H_2O$, $\geq$ 98.0%), Sodium (meta) arsenite ($NaAsO_2$, $\geq$ 90%), tetra-n-butylammonium fluoride trihydrate ($CH_3 (CH_2)_3]_4NF$·$3H_2O$, $\geq$ 97%) and potassium dihydrogen orthophosphate (KH_2PO_4) were purchased from sigma Aldrich, and were used without further purification.

2.2. Instrumentation characterizations for PPy

The obtained material was structurally characterized *via* the following analytical techniques; FTIR; TGA, BET, electrical conductivity and SEM.

The surface area along with the pore size and the volume of PPy was determined using the Brunauer-Emmett Teller (BET) method on COULTER^{TM}SA 3100^{TM} series. Surface area and pore size analyzer (N2 adsorption) with a Gemini apparatus was used. Thermal analysis of PPy was determined using the Thermogravimetric Analyzer TGA Q500 V6.7. N_2 was the purged gas used. Sample was heated 10 ^{0}C to 900 ^{0}C at a heating rate of 10 ^{0}C min^{-1}.

PPy was characterized by infrared spectra using Agilent Cary 600 Series FT-IR spectrometer; the IR spectra were recorded by averaging 32 scans at a spectral resolution of 4 cm^{-1}.

Conductivity measurement has been made after pressing a pellet of PPy using a Kelvin four-point probe technique implemented with a Solar Taron with Z plot and Z view software. For the polymer sample, the thickness, "t", surface area, "s", of the pellets, and the resistance, "R", given by the instrument was used to determine the conductivity. The conductivity, σ (S/cm) is calculated using the following equation:

$$\sigma = t/R \times s \tag{1}$$

Morphological characterization of PPy was carried out using field emission Scanning electron microscope, the samples were suspended in chloroform, and the PPy powder were mounted on a layer of carbon sheet prior to imaging.

2.3. Synthesis and characterization of PPy solid phase extractor

In a 250 mL round bottom flask, pyrrole (2.88 g, 0.043 mol) was suspended in distilled water (100 mL) for few minutes. The flask was placed in an ice bath after which gradual addition of iron (III) chloride hexahydrate (16.25 g, 0.1 mol) dissolved in a 100 mL of water was made to the pyrrole over a period of 15 min. The mixture was left under stirring for 4 h. Black precipitate was observed indicating the termination of the reaction. The product was filtered then washed with cold distilled water and kept in a vacuum oven for 48 h at 35 °C (Scheme 1).

2.4. As (III)-PPy and As(V)-PPy interaction measurements

Following the treatment with arsenic solutions, the solid phase was collected and dried prior to FT-IR measurements. The conformational changes in the functional groups of the PPy upon its interaction with As(III) or As(V) were detected *via* a Fourier Transform Infrared (FT-IR) spectrometer. Spectra of the material of arsenic treated were recorded in the region of 400–4000 cm^{-1} with 32 scans.

A scanning electron microscope (SEM) JEOL JSM-7100F), equipped with secondary and backscattered imaging coupled with UltraDry energy dispersive X-ray (EDX) for elemental analysis was used for morphological investigations. PPy treated with arsenic species samples were mounted in a copper discs known as grid casted with a fine mesh. Samples were run under accelerating voltage of 15 Kev and working distance of 10 mm.

2.5. Arsenic species extraction by PPy

Experiments were carried out to assess the ability of PPy to extract As (III) and As (IV) oxyanions from aqueous solution using
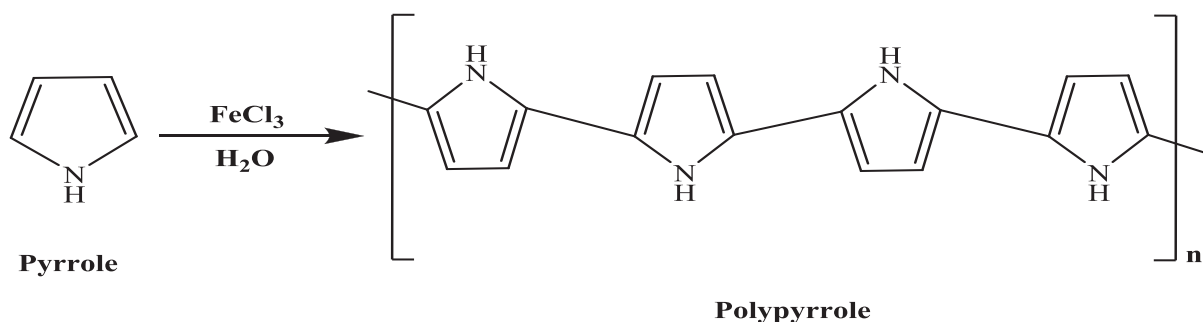
Scheme 1. Synthetic procedure used for the preparation of PPy using FeCl$_3$ as the oxidizing agent.

the batch technique. Parameters tested were the following, the dose effect, pH of the medium, temperature and the interfering ions on the investigated arsenic species extraction by PPy. Uptake capacity of PPy and the kinetics were also investigated.

To investigate the effect of the PPy dose on the extraction process of the tested anions, different masses of the material (0.05–0.25 g) in polypropylene tubes were added to a volume (10 mL) of aqueous As (III) (0.7 ppm; 2.3×10^{-3} mmol L^{-1}) and As (V) (0.7 ppm; 3.6×10^{-3} mmol L^{-1}) solutions. The tubes were agitated on a shaker for 5 min, sealed and kept in a water bath for 18 h at 298 K. Following that, solutions were filtered using Millipore membrane (0.45 μm) and filtrates were analyzed for remaining arsenic concentration. The supernatants were diluted by de-ionized water with no further treatments before their analysis in Agilent 7700x Series Inductively Coupled Plasma Mass Spectrometry, ICP-MS (Agilent Technologies). Calibration curves were completed before the run of the samples with a blank experiment of double de-ionized water (DDW). Analysis was made in triplicate. Removal percentages of arsenic (% Removal of As) were determined according to the Eq. (2)

$$\%\text{Removal of As} = (C_i - C_{eq})/C_i \times 100 \quad (2)$$

In Eq. (2), C_i and C_{eq} denote the initial and the arsenic equilibrium concentrations (mmol L^{-1}) in water.

The pH effect of arsenic salt solutions in aqueous medium on the removal ability of PPy was examined in the 2-10 pH range. The initial concentration of the anions (2.3×10^{-3} mmol L^{-1} of As (III) and 3.6×10^{-3} mmol L^{-1} of As (V)) was kept constant in de-ionized water at the same time as the solution pH was adjusted to the desired values by the addition of 0.1 mol L^{-1} sulfuric acid or 0.1 mol dm^{-3} sodium hydroxide using a digital pH meter (model AB15) equipped with a combined pH electrode. Samples were then left 18 h at 298 K. Afterwards, the supernatants were analyzed for arsenic residual by ICP-MS as described above and the % E was calculated using Eq. (2). The obtained optimal pH was used for further experiments.

To determine whether there is any interference of other anions on the removal of arsenic species from aqueous medium by PPy, solutions with same molar concentrations (1.07 mmol L^{-1}) of multiple anions containing potassium dihydrogen orthophosphate KH_2PO_4, tetra-n-butyl ammonium fluoride trihydrate $C_{16}H_{36}$-FN·$3H_2O$ and sodium arsenate dibasic heptahydrate Na_2HAsO_4-·$7H_2O$ or sodium (meta) arsenite $NaAsO_2$ were prepared in de-ionised water. The remaining concentration was analyzed using ICP-MS.

Uptake capacity of the material to extract As (III) and As (V) was determined using batch experiments. Thus, PPy (0.1 g) was placed in polypropylene tubes containing a volume (10 mL) of different concentrations of arsenic solutions (0.076–1.920 mmol L^{-1} for As (III)) and (0.071–1.7 mmol L^{-1} for As (V)). The mixtures were mechanically agitated for few minutes to reach equilibria. The tubes were then placed in a water bath for 18 h at 298 K. After which anion salts were then analyzed by the ICP-MS.

The uptake capacity, q_{eq} (mmol g^{-1}), per unit mass of the material was calculated using Eq. (3).

$$q_{eq} = \frac{(c_i - c_{eq}) \times v}{m} \quad (3)$$

In Eq. (3), V is the volume (L), C_i and C_{eq} are the initial and the equilibrium arsenic concentrations (mol L^{-1}) respectively, m is the mass of PPy.

To study the temperature effect on the arsenic uptake capacity of PPy, 0.1 g of the material was added to a volume (10 mL) of different concentrations of As(III) or As(V) salt solutions at different temperatures (278, 298 and 323 K). The material was separated by membrane filtration and the remaining concentrations of arsenic in the aqueous solution were determined by ICP-MS. The uptake capacity q_{eq} (mmol g^{-1}) was calculated using Eq. (3).

The kinetics of the arsenic oxyanions removal by PPy was determined using the same conditions described above, but at different time intervals (10–180 min) keeping the solution pH at the optimal arsenic uptake by the material (pH 8 for As (III) and 6.5 for As (V)). The removal capacity q_{eq} (mmol g^{-1}) was calculated, half-life values for removal were determined from the plots of the material uptake capacity (q_{eq}) vs the time in minutes. The following equation for pseudo first order model was applied.

$$\log(Qe - Qt) = logQe - \frac{k_1}{2.303}t \quad (4)$$

Q_e is the maximum removal capacity in mmol g^{-1}, Q_t (mmol g^{-1}) the amount of removal at time (min) and k_1 the Lagergren rate constant of arsenic ions removal (min^{-1}).

3. Analytical Applications

3.1. Material efficiency in real wastewater samples

PPy efficiency as a sorbent was examined using real wastewater samples. These samples were previously analyzed by HPLC for different arsenic organic and inorganic species and ICP-MS for arsenic content after which PPy (0.1 g) was added to 10 cm^3 water samples in plastic tubes. The tubes were kept in a water bath at 298 K for 18 h to equilibrate. Filtrates were analyzed by ICP/MS for arsenic remaining concentration. Percentages of As removed were determined.

3.2. Material in action: Testing real water samples

Different arsenic species were found in Red sea water (Jeddah, Saudi Arabia). Therefore, the removal efficiency of PPy was tested on real water samples analyzed to have different arsenic species with different concentrations (Table 2) collected from three different sites in Red sea.

4. Result and Discussion

4.1. Structural characterizations of the solid phase extractor, PPy

Structural characterization of PPy is a key element in arsenic oxyanions removal process from aqueous medium. The functionalities in the structure along with the material's surface area and morphology will give insights about the mode of its interaction with As (III) and As (V). As far as the PPy electrical conductivity is concerned, Zhang et al. (Zhang et al., 2006) demonstrated the importance of the positively charged nitrogen atoms in enhancing the material's removal capacity to anions.

4.2. Infrared (FT-IR) spectrum and electrical conductivity

The FT-IR spectrum of PPy powder formed by pyrrole oxidation using FeCl$_3$ oxidant is presented in Fig. 1. FT-IR spectrum of PPy reported by several research groups under different polymerization conditions has shown consistent assignments vibration modes (Yağmur, 2020). The peaks at 1540 cm^{-1} and 1448 cm^{-1} correspond to the C=C and N–C stretching vibrations of the pyrrole ring. The peak at 1167 cm^{-1} in the spectrum of PPy is related to the C–C stretching vibration in the pyrrole ring. The band at 1041 cm^{-1} is attributed to the in-plane deformation of N–H bond in the pyrrole ring, 888 and 755 cm^{-1} peaks correspond to C–H out of plane vibrations, 2961 and 2867 cm^{-1} are attributed to the C–H stretching vibrations.
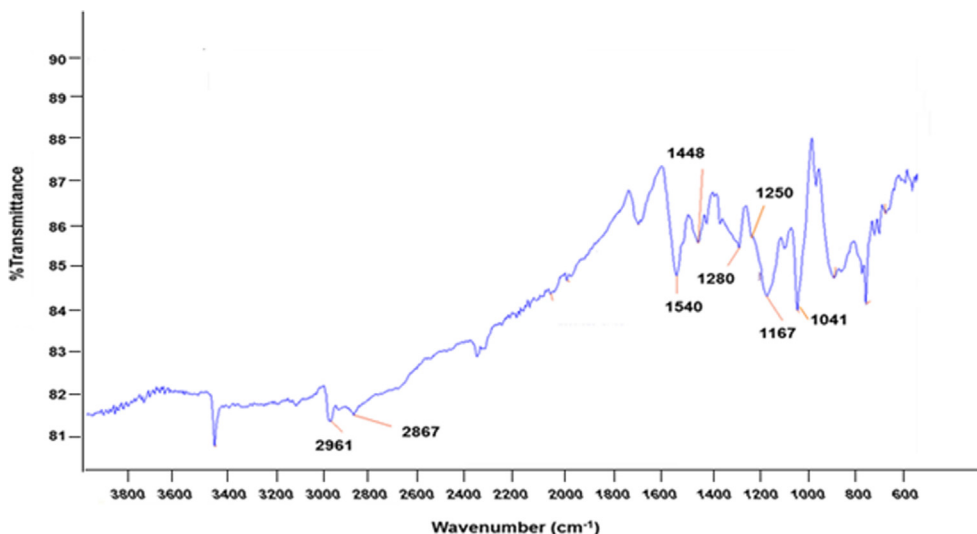
Fig 1. FT-IR spectrum of PPy prepared by FeCl₃.

As far as the electrical conductivity of PPy is concerned, the most values of the chemically prepared material using ferric chloride without adding other additives were <10 S cm^{-1} (Chitte et al., 2011). Alternatively, Machida and co-workers produced a highly conductive PPy (~190 S cm^{-1}) using FeCl₃ in methanol (Machida, 1989). Nevertheless, this value was not reported in other studies. Regarding the electrical conductivity of the prepared PPy, a conductivity value of 6.83 S cm^{-1} under air atmosphere was obtained. This can be due to its hygroscopic nature when it was exposed to atmospheric laboratory conditions. Supposedly, oxygen defects were provoked in the presence of water during the oxidative polymerization of pyrrole through which they led to a decrease in the PPy electrical conductivity (Yağmur, 2020).

4.3. Thermal studies (TGA) of PPy

Fig. 2 shows the variation of weight loss as a function of temperature. In other terms, PPy loses from its weight as temperature increases. This process occurs as a result of releasing volatiles at

high temperatures and product degradation. From the thermogram, an initial 9.4% weight loss that is due to the release of water physically adsorbed on the surface and this represents the first break in the TGA curve which took place between 25 and 100 ^{0}C. Second degradation started at 100 ^{0}C and it continued with slow decomposition to 450 ^{0}C during which about 18% of mass was lost and this is attributed to the degradation of the excess pyrrole material. The third and the fourth breaks in the TGA curve correspond to the degradation of the polymer. This pointed out that the PPy is stable up to a temperature of about 450 ^{0}C.

4.4. BET and scanning electron microscope (SEM) analyzes of PPy

PPy surface area is considered to be an important parameter in the interaction process with the arsenic oxyanion species. Typical BET inset is presented in Fig. 3. Inspection of the figure shows that the adsorption and desorption branches of the isotherms do not coincide, resulting in the formation of the H₄ hysteresis loop. The shape of the hysteresis loop presents information of pore struc-
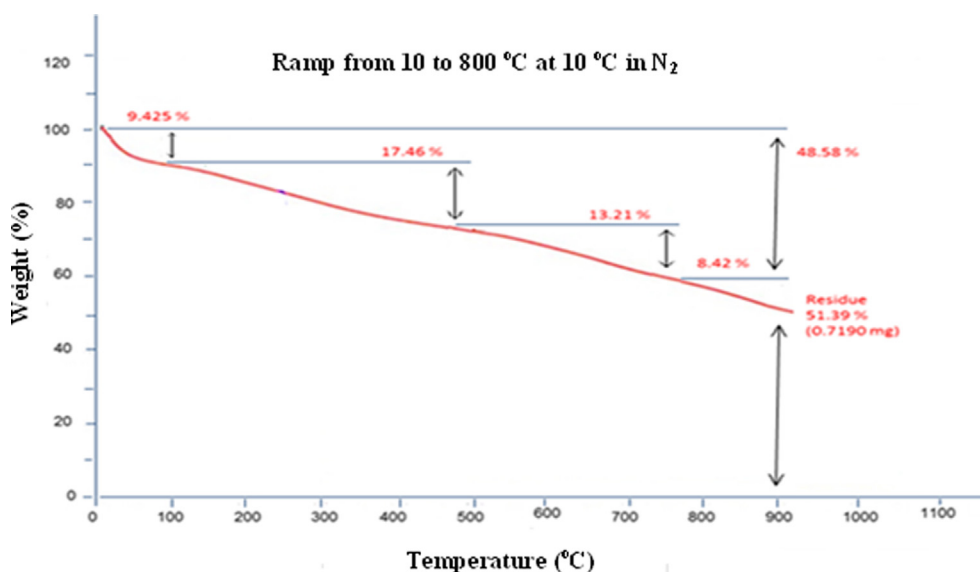

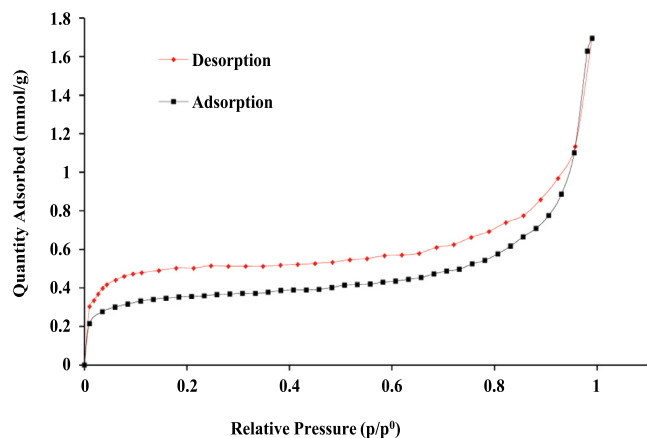**Fig 2.** Thermogram of PPy prepared by chemical method.

Fig 3. Adsorption/desorption isotherms of PPy.

tures. The isotherm was identified as type IV isotherm which is an indicator of mesoporous structure. Based on the BET analysis of PPy, the surface area, pore volume, pore size and particle size were found to be 37.6987 ± 0.8686 m^2 g^{-1}, 0.0122 cm^3 g^{-1}, 62.39 Å and $\sim 4.1–6.5$ μm respectively. In an attempt to corroborate it further, SEM on the sample was carried out as discussed below.

The PPy micrographs show a granular morphology with many pores and cavities (Fig. 4a and b). This finding means that the chemical condensation mechanism of the PPy is realized. The granules have an average size of ~4.1–6.5 μm. The SEM result confirms the mesoporosity structure of the PPy as obtained by BET analysis.

4.5. FT-IR and SEM-EDX measurements for as (III) and as (V) interaction with PPy

FT-IR measurements were carried out for As (III) and As (V) oxyanions loaded PPy. Shifts in the material characteristic bands as a result of As (III) and As (V) oxyanions interaction are presented in Table 1. Inspection of the vibrational frequencies of As (III)-PPy and As (V)-PPy **interaction** reveal red shift in the N–H functionality from 1041 cm^{-1} to 1027 and 1022 cm^{-1} respectively indicating an interaction between the arsenic species oxygen group and NH proton of the PPy *via* hydrogen bond formation. Small shifts in the peaks attributed to the C-N and C = C stretching vibrations in the pyrrole ring were observed. This is due to the deformation in the pyrrole ring and consequently shifting the material characteristic bands.

SEM provides the spatial resolution of the analyzed sample whereas EDX generates its elemental composition. PPy was analyzed using SEM-EDX prior and after being in contact with arsenic oxyanions in aqueous solution where micrographs with EDX spectra are shown in Fig. 5. The solid part was analyzed by SEM, and the elemental composition was detected by energy dispersive atomic X-ray. As shown in the SEM micrographs, the morphology of PPy appears to be little different after its interaction with As (III) and As(V) oxyanions. As it was obtained by the EDX spectra, arsenic peak was found among the elemental composition of PPy (Fig. 5b and c) and this confirms its presence in the PPy samples.

4.6. Extraction of As(III) and As(V) species in water

Due to the one-step synthesis and environmental stability, PPy has been considered as a good candidate for arsenic sorption (Abdi et al., 2009). Besides, the NH functionality in its structure can boost its selectivity for arsenic oxyanions through hydrogen bond formation. The material was used as a solid-phase for the uptake of As (III) and As (V) from water due to its undetected solubility in water as previously reported in the literature (Lee et al., 2000). This part of the study presents the approaches of the sequential optimization process. Different variables were selected to conduct the optimization process as described in the Materials and Methods Section.
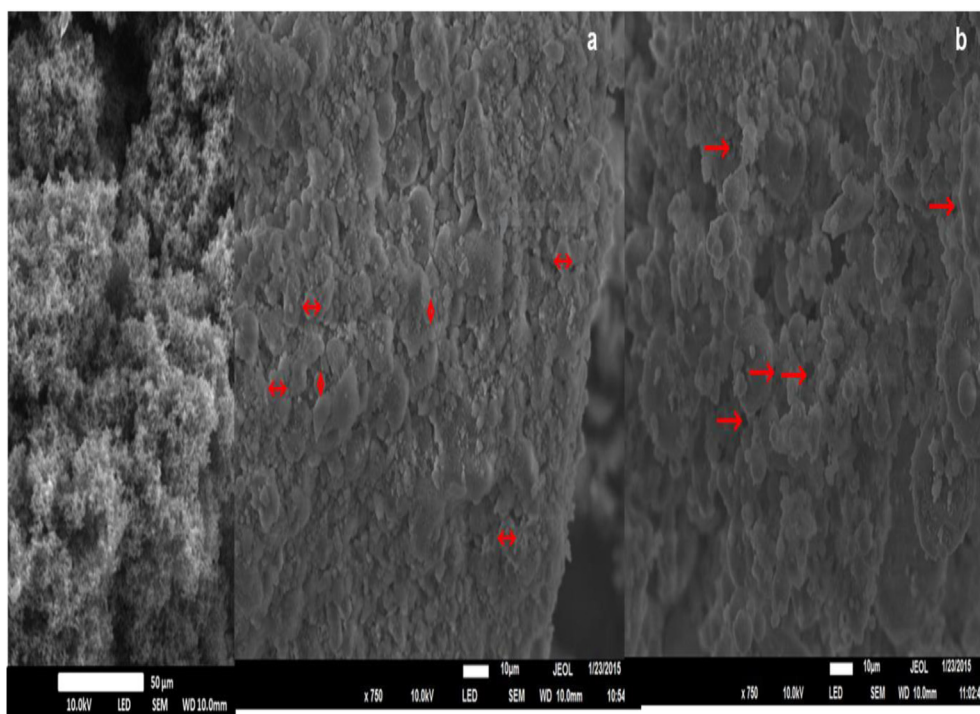

Fig 4. Scanning electron micrographs of PPy showing a granular (a) and porous (b) morphology.

Table 1
Infrared band absorption frequencies (cm^{-1}) of arsenic- PPy complexes.

PPy Wavenumber (cm^{-1})	As (III)-PPy Wavenumber (cm^{-1})	As (V)-PPy Wavenumber (cm^{-1})	Vibrational Assignments
1540	1532	1531	C = C stretching of pyrrole ring
1448	1445	1444	C-N stretching vibration in the ring
1167	1141	1142	C–C stretching vibration in the ring
1041	1027	1022	N–H in plane deformation
888	840	838	C–H out plane vibration
755	704	700	C–H out of plane vibration
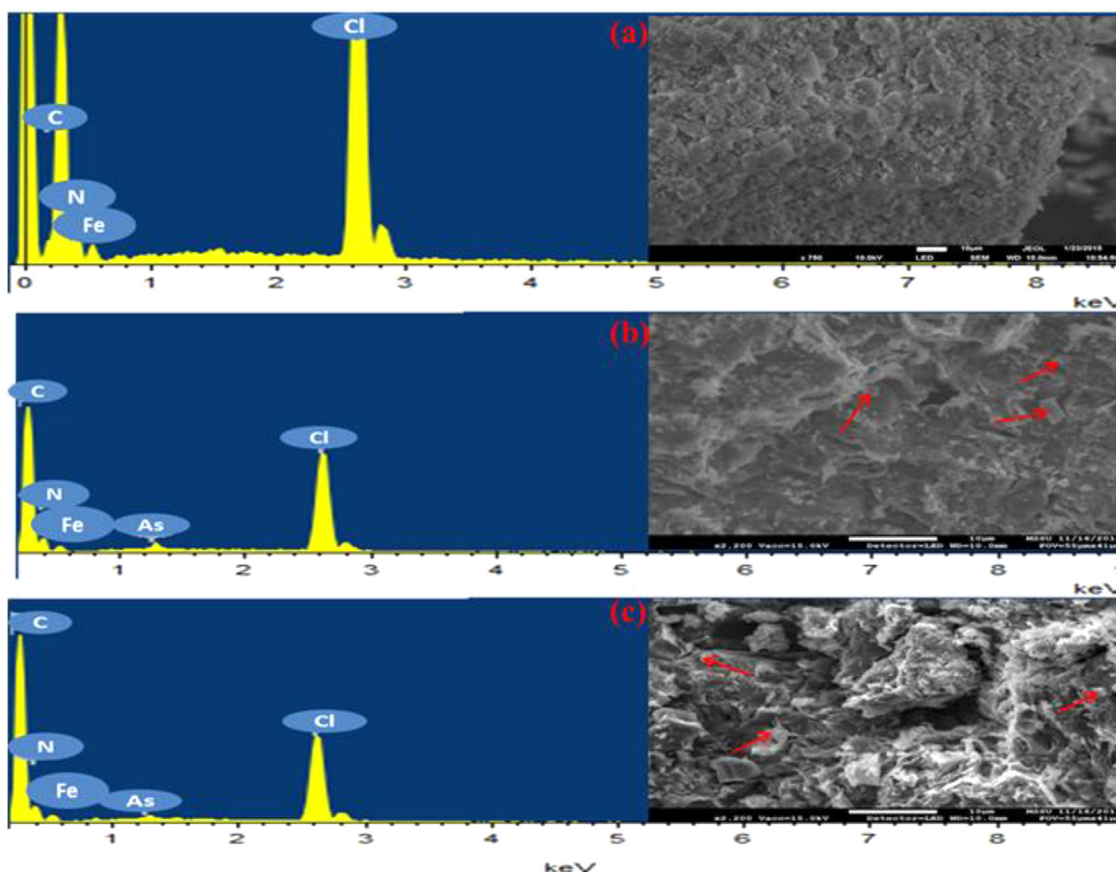
Fig 5. Scanning electron micrographs along with EDX spectra showing the morphology and the composition of PPy (a); PPy loaded with As (III) (b); PPy loaded with As (V) (c). Fe and Cl elements refer to the excess oxidant in the samples.

The result (% Removal of As) is shown in Fig. 6. It can be observed that the removal capability of PPy to sequester arsenic oxyanions from aqueous medium gradually increased with material mass increase until nearly saturation state was reached. However, the highest removal of As (III) and As (V) was attained at 0.1 g PPy. Further additions of PPy did not yield significant variation in the arsenic oxyanions removal. This indicates that all the NH moieties, the binding sites in PPy have been occupied by the arsenic oxyanions (Danil de Namor et al., 2017). The results show that the optimum mass of PPy to remove arsenite and arsenate oxyanions from water was 0.1 g for a volume of 10 cm^3 of the aqueous solution as the highest percentage (%) of As (III) and As (V) removal was obtained.

Arsenic speciation is highly reliant on the pH of the aqueous environment. Its speciation in aqueous medium is controlled by the pH of the solution resulting in different ionic species. Moreover at high pH, higher concentration of hydroxyl anions can be aggressive competitors for the material exchange sites (Danil de Namor et al., 2017).

The pH effect on the ability of PPy to remove As (III) and As (V) oxyanions was investigated over a range of 2–10. As presented in
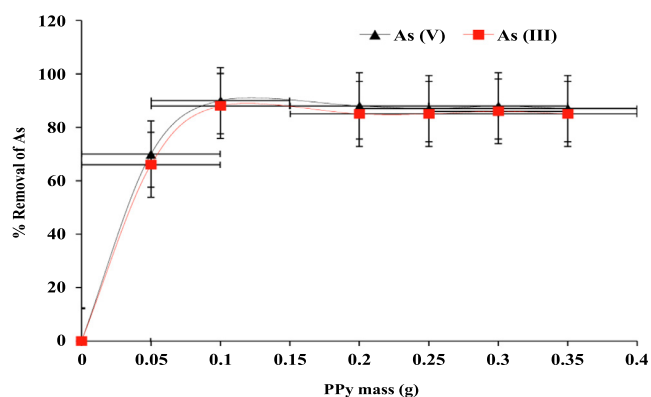

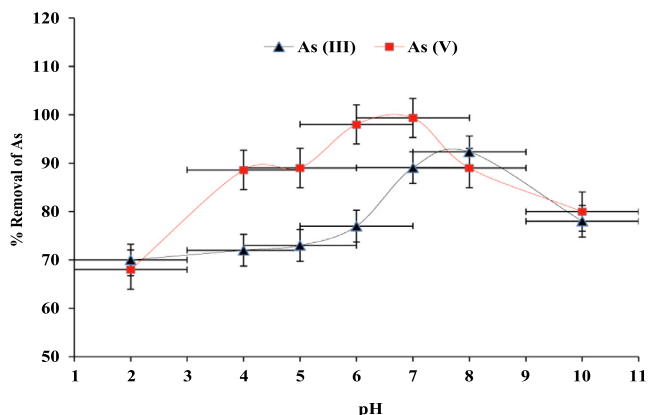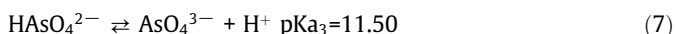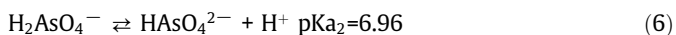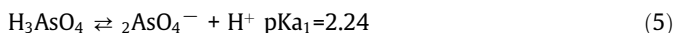**Fig 6.** Effect of mass of the PPy on the removal of As (III) and As (V) oxyanions at 298 K.

Fig 7. pH effect on As (III) and As (V) oxyanions removal by PPy at 298 K.

Fig. 7, the percentage (%) of As removed by PPy were plotted against the solution pH. The analysis of the data showed that the sorption of As(III) and As(V) oxyanions highly depends on the pH of the medium. The optimum pH for maximum As(III) removal was attained at pH 8 whereas pH 6.5 was the optimum for As(V) after which arsenic removal decreased at higher pH values due to the competition between the hydroxyl anions and the arsenic oxyanions to the material binding site.

To illustrate the effect of solution pH on the removal ability of PPy, pK$_a$ values for the sequential arsenic acid dissociation in water at 298 K are considered as follow (Dean, 1979)

$$H_3AsO_4 \rightleftharpoons {}_2AsO_4{}^- + H^+ \quad pKa_1 = 2.24 \tag{5}$$

$$H_2AsO_4{}^- \rightleftharpoons HAsO_4{}^{2-} + H^+ \quad pKa_2 = 6.96 \tag{6}$$

$$HAsO_4{}^{2-} \rightleftharpoons AsO_4{}^{3-} + H^+ \quad pKa_3 = 11.50 \tag{7}$$

Arsenite in water occurs only in the form of arsenous acid H$_3$-AsO$_3^0$also known as As(OH)$_3^o$ (neutral arsenite), with pKa$_1$ value < 9.23 that is less than pH 9 which was the obtained optimal pH value as shown in Fig. 7. Regarding arsenate and polypyrrole, the percentage removal of the species by the material increased up to pH 6.5 with HAsO$_4^-$predominating the solution after which a decrease in removal percentage was obtained due to the increased amount of HAsO$_4^{2-}$ in solution.

The competing effect of fluoride and phosphate ions on As (III) and As (V) species uptake by PPy was examined in aqueous medium. It was clearly observed the inhibitory effect of fluoride and phosphate ions on As(III) and As(V) uptake by PPy, in a way that the percentage (%) of As (III) removed by PPy decreased from 88 to 76%, while that for As(III) was reduced from 90% to 79%.

The uptake capacity of PPy is displayed in Fig. 8 where the mmol of arsenic species uptake per unit mass of the material (mmol g^{-1}) is presented versus the arsenic oxyanions equilibrium concentration (mmol L^{-1}). As presented in the plot, gradual increase in PPy capacity was obtained with arsenite and arsenate concentrations increase until equilibrium was reached. This refers to the saturation of NH active sites with the arsenic oxyanions
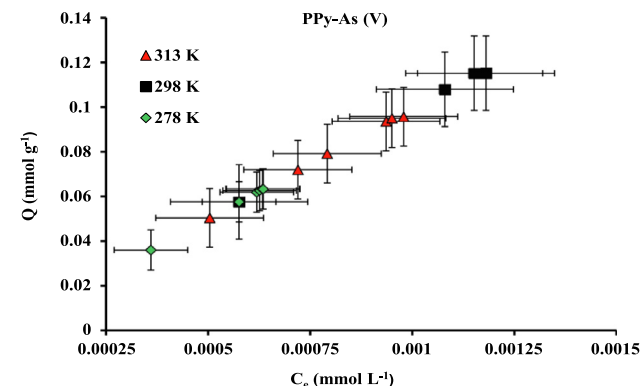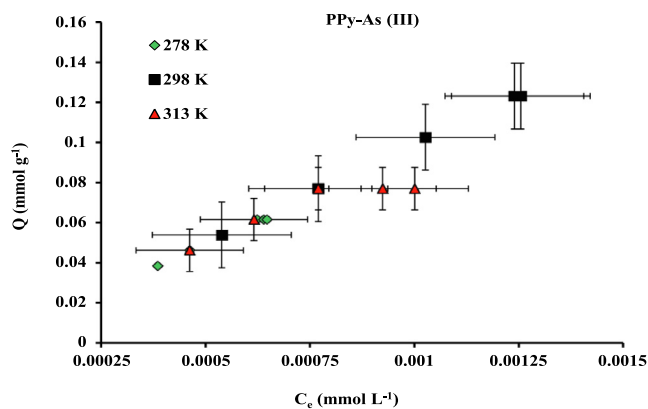

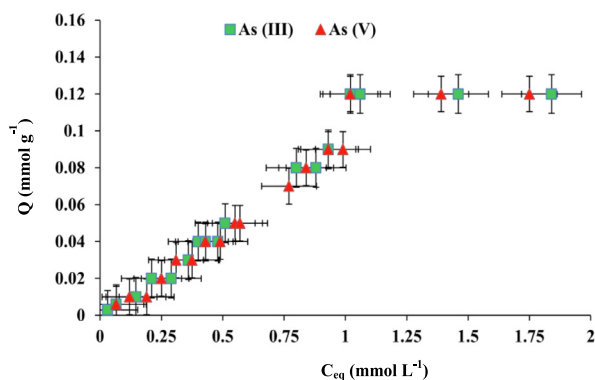**Fig 9.** Effect of temperature on As (III) and As (V) uptake capacity of PPy; pH 8 for As (III); pH 6.5 for As (V).

Fig 8. Uptake capacity of PPy for As(III) and As(V) oxyanions at 298 K. pH 8 for As (III); pH 6.5 for As (V).
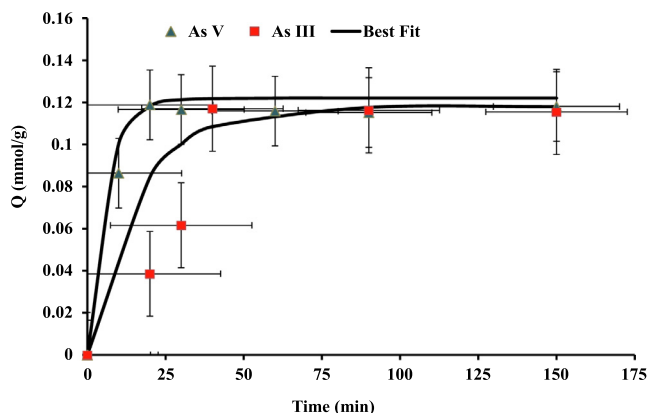

Fig 10. Contact time effect on As (III) and As (V) oxyanions uptake from water by PPy at 298 K; pH 8 for As (III); pH 6.5 for As (V).

Table 2
Percentages of arsenic species removed from collected wastewater samples.

Site	Found Arsenic species	Arsenic Initial Concentration ($\mu g\ L^{-1}$)	Arsenic Final Concentration ($\mu g\ L^{-1}$)	Arsenic Extracted (%)
Ligand: PPy				
S1	As (III) (60%), As (V), (18%), Monomethyl Arsenic (4%) & Dimethyl Arsenic (1%)	243 ± 0.7	4.24 ± 0.4	98.25
S2	Arsenate, As (V)	141.5 ± 0.2	2.06 ± 0.6	98.53
S3	Arsenate, As (V)	200 ± 0.8	2.26 ± 0.5	98.86
S4	As (III) (70%), As (V) (7%), & Methylated Arsenic (13%)	360 ± 0.3	4.55 ± 0.4	98.73

* The results are based on three replicate measurements; Ligand mass/Volume (g/mL): 0.1/10; pH 6.7.

Table 3
Comparative evaluation of some used materials in the removal of arsenic from aqueous system.

Material	As (III) Capacity ($mg\ g^{-1}$)	As (V) Capacity ($mg\ g^{-1}$)	Reference
PPy	15.58	16.67	This study
PPy	–	1.91	Obidul Huq et al., 2018
PPy- greigite (Fe3S4) nanocomposites	8.61	8.72	Islam and Patel, 2017
PPy-Nickel nanocomposites	2.64	-	Srivastava et al., 2016
Calix[4]pyrrole	14.29	15.28	Danil de Namor et al., 2017
Mg-Fe-ClLDH	14.6	-	Jiang et al., 2015
Fe-Montmorillonite	–	> 0.019	Iriel et al., 2014
Goethite	–	0.48	Garrido and Romero, 2014
Siderite-coated sand	–	0.52	Wang et al., 2018
Haematite-coated sand	–	2.37	Dai et al., 2016
Activated carbon	29.9	30.48	Pattanayak et al., 2000
Red mud (ARM)	0.88	0.94, 2.28	Roy et al., 2020
Humic acid	–	1.98	Devaraj et al., 2019

(Danil de Namor et al., 2017). The results show that the capacity of PPy to remove As (III) and As (V) was 0.12 mmol g^{-1} or 15.58 mg g^{-1} for As (III) and 16.67 mg g^{-1} for As (V).

The effect of temperature on the removal capacity of PPy was investigated under optimum conditions where mmol of arsenic salts per unit mass of the material versus the C_{eq} of As (III) and As (V) species in mmol L^{-1} is displayed in Fig. 9. The obtained findings indicate no significant variations in the removal capacity with different temperatures. The fact is the removal process depends on the material binding sites rather than the temperature of the system (Danil de Namor et al., 2017).

The time required to attain equilibrium was investigated as it is important to explore the kinetics of the extraction process, particularly for commercial applications. Thus, Fig. 10 displays the removal capacity data (mmol g^{-1}) for the investigated arsenic species versus time (min). The rate of removal of these oxyanions and the half-life of the processes were calculated from the amount of data available over the region going from zero to maximum. The As (III) and A (V) maximal removal by PPy reached the equilibrium within the first 40 min.

By fitting the data points, the half –life ($t_{1/2}$) which represents the operating period to attain 50% of the complete removal process and equilibrium rate constants (k) are as follows,

As (III) $t_{1/2}$: 11 min; k=: 0.062 min^{-1} and As (V) $t_{1/2}$: 4 min; k = 0.17 min^{-1}. From the computed data, it was observed that the removal of As (III) and As (V) oxyanions mechanisms by PPy fitted to the pseudo first order kinetic model. The findings came with good agreement with previously reported studies on the removal of As (III) by iron oxide impregnated activated alumina and As (V) by PPy (Obidul Huq et al., 2018). These results demonstrate that the removal process is fast, an important issue to consider for commercialization purposes.

4.7. Ppy efficiency on real samples

The efficiency of PPy as an extracting agent against arsenic species removal was investigated using real water samples contaminated with organic and inorganic arsenic species.

The percentages of these species along with the total arsenic initial (C_i) and equilibrium (C_{eq}) concentrations and the percentage (%) of arsenic removed by PPy are given in Table 2. The 98% removal ability of PPy proves its effectiveness as an extracting material for arsenic different species (organic and inorganic) and for its use in large scale application.

5. Comparative study with other used arsenic extracting agents

The commonly used technologies in arsenic ions removal from wastewaters are adsorption onto activated alumina, zeolites (Camerotto Andreanii et al., 2014), pillared clay (Iriel et al., 2014) and precipitation or adsorption using metal oxides, mostly iron based sorbents (Fiúza et al., 2014) like zerovalent iron nanoparticles (Fiúza et al., 2014), granular ferric hydroxide oxide (Pintor et al., 2018), goethite (FeO(OH)) (Tufo et al., 2014), and membranes in addition to the employment of macrocycles (Danil de Namor et al., 2017).

The uptake capacity of PPy in this present study is high compared to the previously reported studies using the same material or its composites as shown in Table 3.

Despite the high capacity of the activated carbon reported by Pattanayak et al. (2000), the preparation of these samples is time consuming.

Bi-metal adsorbents such as Iron Zirconium oxide (Ren et al., 2011), Mn-oxide-doped Al oxide (Wu et al., 2012) were also used as a method for the removal of arsenic from water. These materials showed high capacity for the removal of arsenic, but some of these materials require multistep synthesis procedure and the initial concentration of arsenic for the batch experiments was ranging from 5 − 300 mg L^{-1} only.

6. Conclusions

The results demonstrate that PPy is a suitable de-contaminating agent for the removal and recovery of As(III) and As(V) oxyanions from water. The optimal pH study suggests that the material can

be recycled at low pH (pH switching mechanism). The obtained capacity of PPy for As(III) and As(V) was 15.58 and 16.67 mg g^{-1} respectively. The PPy effectiveness over real water samples containing organic and inorganic arsenic species with 98% arsenic removal propose its employment in Pilot Plant scale to decontaminate arsenic species from water.

Declaration of Competing Interest

The author declares that they have no known competing financial interests or personal relationships that could have appeared to influence the work reported in this paper.

Acknowledgements

References

Abdi, M.M., Kassim, A., Mahmud, H.N.M.E., Mat Yunus, W.M., Talib, Z.A., Sadrolhosseini, A.R., 2009. Physical, optical, and electrical properties of a new conducting polymer. J. Mater. Sci. 44 (14), 3682–3686. https://doi.org/10.1007/s10853-009-3491-y.

Ansari, R., Feizy, J., Delavar, A.F., 2008. Removal of arsenic ions from aqueous solutions using conducting polymers. E.-J. Chem. 5 (4), 853–863. https://doi.org/10.1155/2008/908937.

Armes, S.P., 1987. Optimum reaction conditions for the polymerization of pyrrole by iron (III) chloride in aqueous solution. Synthetic Metals 20, 365–371. https://doi.org/10.1016/0379-6779(87)90833-2.

Barakat, M.A., Ismat-Shah, S., 2013. Utilization of anion exchange resin Spectra/Gel for separation of arsenic from water. Arabian J. Chem. 6 (3), 307–311. https://doi.org/10.1016/j.arabjc.2010.10.011.

Camerotto Andreanii, P.A., Trinelli, M.A., Leal, P.R., Rodriguez, A.V., Rodriguez, A.I., Llano, J., Dos Santo Afonso, M., 2014. CRC Press, Taylor and Francis Group London, ISBN 978-1-138-00141-1.

Capito, P., Xu, M., Cath, T.Y., 2013. Selective removal of arsenic and monovalent ions from brackish water reverse osmosis concentrate. J. Hazard. Mater. 260, 885–891. https://doi.org/10.1016/j.jhazmat.2013.06.038.

Chitte, H., Shinde, G., Bhat, N., Walunj, V.,, 2011. Synthesis of Polypyrrole Using Ferric Chloride (FeCl$_3$) as Oxidant Together with Some Dopants for Use in Gas Sensors. Journal of Sensor Technology 1, 47–56. https://doi.org/10.4236/jst.2011.12007.

Dai, M., Xia, L., Song, S., Peng, C., Lopez-Valdivieso, A., 2016. Adsorption of As(V) inside the pores of porous hematite in water. J. Hazard. Mater. 307, 312–317. https://doi.org/10.1016/j.jhazmat.2016.01.008.

de Namor, A.F.D., Hakawati, N.A., Hamdan, W.A., Soualhi, R., Korfali, S., Valiente, L., 2017. Calix[4]pyrrole for the removal of arsenic (III) and arsenic (V) from water. J. Hazard. Mater. 326, 61–68. https://doi.org/10.1016/j.jhazmat.2016.11.066.

De Klerk, R.J., Jia, Y., Daenzer, R., Gomez, M.A., Demopoulos, G.P., 2012. Continuous circuit coprecipitation of arsenic(V) with ferric iron by lime neutralization: process parameter effects on arsenic removal and precipitate quality. Hydrometallurgy 111-112, 65–72. https://doi.org/10.1016/j.hydromet.2011.10.004.

Dean, J.A., 1979. Lange's Handbook of Chemistry. Mc Graw-Hill, New York, NY.

Devaraj, N.K., Elghazali, S.R., Ganapathe, L.S., Mukter-Uz-Zaman, A.S.M., Wong, H.Y., 2019. As(V) adsorption kinetics of humic acid-coated magnetite particles. Appl. Mech. Mater. 892, 72–78.

Fiúza, A., Futuro, A., Guimarães, M., 2014. CRC Press, Taylor and Francis Group London, ISBN 978-1-138-00141-1.

Garrido, S.E., Romero, L., 2014. CRC Press, Taylor and Francis Group London, ISBN 978-1-138-00141-1.

Herbel, M., Fendorf, S., 2006. Biogeochemical processes controlling the speciation and transport of arsenic within iron coated sand. Chem. Geol. 228, 16–32.

Iriel, A., Fernández, C.A., Marco-Brown, J.L., Trinelli, M.A., Pérez, A.L., dos Sanotos Afonso, M., 2014. CRC Press, Taylor and Francis Group London, ISBN 978-1-138-00141-1.

Islam, M., Patel, R., 2017. Solvothermal synthesis of greigite (Fe 3 S 4)– conducting polypyrrole nanocomposite and its application towards arsenic removal. Sep. Sci. Technol. 52 (18), 2837–2854. https://doi.org/10.1080/01496395.2017.1377247.

Jiang, J.-Q., Ashekuzzaman, S.M., Hargreaves, J.S.J., McFarlane, A.R., Badruzzaman, A.B.M., Tarek, M.H., 2015. Removal of Arsenic (III) from groundwater applying a reusableMg-Fe-Cl layered double hydroxide. J. Chem. Technol. Biotechnol. 90, 1160–1166.

Lee, Y.H., Lee, J.Y., Lee, D.S., 2000. A novel conducting soluble polypyrrole composite with a polymeric co-dopant. Synth. Met. 114 (3), 347–353. https://doi.org/10.1016/S0379-6779(00)00268-X.

Litter, M., Nicolli, H., Meichty, M., Quici, N., Bundschuh, J., Bhattacharya, P., Naidu, R. (Eds.). 2014. In: Proceedings 5th Internat. Congress on Arsenic in the Environment, Buenos Aires, Argentina.

Machida, S., Miyata, S., Techagumpuch, A., 1989. Chemical synthesis of highly electrically conductive polypyrrole. Synthetic Metals 31, 311–318. https://doi.org/10.1016/0379-6779(89)90798-4.

Obidul Huq, A.K., Yahya, R., Ekramul, H.N.M., 2018. Equilibrium, kinetics, and thermodynamics studies of polypyrrole adsorbent for arsenic ions. Water Sci. Tech.-W Sup. 18 (1), 240–250.

Pattanayak, J., Mondal, K., Mathew, S., Lalvani, S.B., 2000. A parametric evaluation of the removal of As (V) and A s(III) by carbon-based adsorbents. Carbon 38, 589–596.

Pintor, A.M.A., Vieira, B.R.C., Santos, S.C.R., Boaventura, R.A.R., Botelho, C.M.S., 2018. Arsenate and arsenite adsorption onto iron-coated cork granulates. Sci. Total Environ. 642, 1075–1089.

Ren, Z.M., Zhang, G.S., Paul, C.J., 2011. Adsorptive removal of arsenic from water by an iron–zirconium binary oxide adsorbent. J. Colloid Interface Sci. 358, 230–237.

Roy, J.S., Bhattacharya, G., Chauhan, D., Deshmukh, S., Upadhyay, R., Priyadarshini, R., Roy, S.S., 2020. Potential use of smartly engineered red mud nanoparticles for removal of arsenate and pathogens from drinking water. SN Appl. Sci. 2, 796–807.

Singh, T., Pant, K., 2004. Equilibrium, kinetics and thermodynamic studies foradsorption of As(III) on activated alumina. Sep. Purif. Technol. 36, 139–147.

Shankar, S., Shanker, U., Shikha, 2014. Arsenic contamination of groundwater: a review of sources, prevalence, health risks, and strategies for mitigation. Sci. World J. 304524.

Smedley, P.L., Kinniburgh, D.G., 2002. A review of the source, behaviour and distribution of arsenic in natural waters. Appl. Geochem. 17 (5), 517–568.

Srivastava, S.K., Senapati, S., Singh, S.B., Raul, P.K., 2016. Magnetic Ni/PPy nanocomposite as effective reusable adsorbent for removal of arsenite and fluoride from contaminated water. RSC Adv. 6, 113424–113431.

Tufo, A.E., Marchi, M.C., Dos Santo Afonso, M., Sileo, E.E., Landi, S.M., 2014. CRC Press, Taylor and Francis Group London, ISBN 978-1-138-00141-1.

Tyson, J., 2013. The determination of arsenic compounds: a critical review. ISRN Anal. Chem. 2013, 1–24.

Wang, Z., Ma, T., Zhu, Y., Abass, O.K., Liu, L., Su, C., Shan, H., 2018. Application of siderite tailings in water-supply well for As removal: experiments and field tests. Int. Biodeterior. Biodegrad. 128, 85–93.

WHO, 2010. Exposure to Arsenic: A Major Public Health Concern. Preventing Disease Through Healthy Environments [on-line]. http://www.who.int/ipcs/features/arsenic.pdf (accessed July 2016).

Wu, K., Liu, T., Xue, W., Wang, X., 2012. Arsenic (III) oxidation/adsorption behaviors on a new bimetal adsorbent of Mnoxide-doped Al oxide. Chem. Eng. J. 192, 343–349.

Wysocka-Zolopa, M., Goclon, J., Basa, A., Winkler, K., 2018. Polypyrrole nanoparticles doped with fullerene uniformly distributed in the polymeric phase: synthesis, morphology, and electrochemical properties. J. Phys. Chem. C 122, 25539–25554.

Xia, S., Dong, B., Zhang, Q., Xu, B., Gao, N., Causseranda, C., 2007. Study of arsenic removal by nanofiltration and its application in China. Desalination 204, 374–379.

Yağmur, H.K., 2020. Synthesis and characterization of conducting polypyrrole/bentonite nanocomposites and in-situ oxidative polymerization of pyrrole: adsorption of 4-nitrophenol by polypyrrole/bentonite nanocomposite. Chem. Eng. Commun.

Zhang, X., Bai, R., Tong, Y.W., 2006. Selective adsorption behaviors of proteins on polypyrrole-based adsorbents. Sep. Purif. Technol. 52, 161–169.